ELSEVIER

International Journal of Heat and Fluid Flow 23 (2002) 308–316

International Journal of HEAT AND FLUID FLOW

www.elsevier.com/locate/ijhff

Two-phase heat transfer on an isothermal vertical surface: a numerical simulation ☆

Farzad Bazdidi-Tehrani *, Saeed Zaman

Department of Mechanical Engineering, Iran University of Science and Technology, Narmak, Tehran 16844, Iran

Abstract

The present work is aimed at studying the two-phase heat transfer, concerning the film boiling process on an isothermal vertical surface, through the bubble growth mechanism by a numerical simulation of the evolution of the vapor–liquid interface. The interface is captured by a level set method, which is modified to include the liquid–vapor phase change effect. The phase change effect and mass transfer at the interface have been considered in the continuity equation. Also, the gravity and surface tension effects have been taken into account in the momentum equation. The fluid flow adjacent to the hot surface was assumed as laminar, unsteady and two-dimensional. The governing continuity, momentum and energy equations, which include the spatial and temporal changes, and also the interface evolution equation, have been solved by a finite difference numerical method, which has implemented the TDMA algorithm and the projection method. Then, the velocity and temperature fields and also the interface location have been computed. The present numerical results are compared with the available experimental data and with the analytical predictions, which have showed to be in reasonable agreements. © 2002 Published by Elsevier Science Inc.

Keywords: Two-phase; Film boiling; Numerical simulation; Interface; Modified level set method

1. Introduction

Considerable amounts of work have been carried out in the last few years to understand the interface dynamics associated with the phase change process, namely the film boiling and condensation. Because of the complicated behavior of the film boiling phenomenon, all of the investigations made on this topic, before the end of 1990s, were based on experimental methods or analytical models, with many simplifying assumptions.

The first theoretical analysis of the film boiling phenomenon was reported by Bromley (1950). He described saturated natural convection film boiling on horizontal cylinders, in terms of a laminar steady vapor film flowing between the heating surface and the liquid.

Greitzer and Abernathy (1972) presented an empirical-analytical model of natural convection film boiling on a vertical surface. In their model, the interface waves effect was taken into account and the vapor flow was assumed as unsteady and laminar. They stated that the interface waves were moving upward with constant velocity, so they adopted coordinates fixed to the wave system. Thus the phenomenon became steady and the liquid far from the heated surface moved downward with the same velocity, as shown in Fig. 1. Also, the vapor layer consisted of large bulges and thin films. They assumed that the heat transfer in the large bulges was negligible, so the total heat transfer between the hot surface and liquid bulk was referred to the thin films. Finally, they used scaling methods to evaluate the mass, force and energy balances and then, based on some experimental data and through the extrapolation methods, the scaling correlation was converted to the exact equation.

Bui and Dhir (1985) reported an analytical model, based on experimental observation for the film boiling on a vertical surface. They reported that the liquid–vapor interface was unsmooth and combined with large and small scale waves. Also, the order of magnitude of wavelength for large scale waves was in centimeters and the amplitude of these waves was changed with distance from the lower edge of surface. However, the small scale

☆ This paper is a revised and expanded version of a paper presented at CHT'01, the Second International Symposium on Advances in Computational Heat Transfer (Palm Cove, Qld., Australia, 20–25 May 2001), the proceedings of which were published by Begell House, Inc.

* Corresponding author.
E-mail address: bazdid@iust.ac.ir (F. Bazdidi-Tehrani).

0142-727X/02/$ - see front matter © 2002 Published by Elsevier Science Inc.
PII: S0142-727X(02)00178-9

Nomenclature

C_P	specific heat
g	gravity vector
Gr	Grashof number, $(\rho_v g\lambda_0^3/\mu_v^2)(\rho_l/\rho_v - 1)$
H	step function
h_{fg}	latent heat of evaporation
h	mesh size
K	thermal conductivity
k	interfacial curvature
m	mass flux vector
Nu	Nusselt number, $\partial T^*/\partial Y^*\|_{Y^*=0}$
Pr	Prandtl number, $C_{pv}\mu_v/K_v$
P	pressure
S_P	super heat parameter, $C_{Pvf}\Delta T/h_{fg}$
S_p^*	modified super heat parameter, $S_P/(1 + 0.5S_P)$
T	temperature
ΔT	temperature difference, $T_W - T_{SAT}$
U	velocity vector
U_i	interfacial velocity vector
u, v	x- and y-direction velocity component
Δx, Δy	x- and y-direction mesh size

Greeks

λ_0	Laplace capillary length, $[\sigma/g(\rho_l - \rho_v)]^{1/2}$
$\lambda_{d,KH}$	most dangerous Kelvin–Helmholtz wavelength
μ, v	dynamic, kinematic viscosity
ρ	density
σ	surface tension
ϕ	level set function

Subscripts

fg	difference between vapor–liquid properties
i	interface
l, v	liquid, vapor
SAT, W, f, atm	saturation, wall, film, atmosphere
vf	vapor at film temperature
t, x, y	partial differentiation with respect to t, x, y

Superscripts

n	old time step
$n + 1$	new time step
$*$	middle time step, modified

waves had a much smaller wavelength and their amplitude was only a percentage of mean vapor film thickness. In this model, similar to the previous one, the area adjacent to the hot surface was divided into two regions. The first region was the thin vapor film which occupied the distance between the bulges of vapor. In this region, the vapor film was very thin. So, to evaluate the momentum equations, the effects of inertia forces could be neglected and only buoyancy and viscosity terms would be considered. The second region consisted of the hot surface areas which were covered with vapor bubbles. However, the heat transfer rate in this region was low, compared with the first region, but as the significant area of the hot surface was covered with vapor bubbles, therefore the effect of heat transfer in this region could not be neglected. Also, they assumed that the effects of flow in the vapor bubbles were negligible and only the conduction heat transfer was considered in this region. Finally, they derived the heat transfer coefficient as a mean value over the two mentioned regions.

One of the more recent investigations in film boiling on a vertical surface was made by Nishio and Ohtake (1993). In their study, a new method known as vapor-unit-film model was developed to evaluate the heat transfer in natural convection film boiling. The vapor film adjacent to the vertical surface was combined from two sections, according to Fig. 2. The first section was the down edge of surface with steady vapor flow, so that

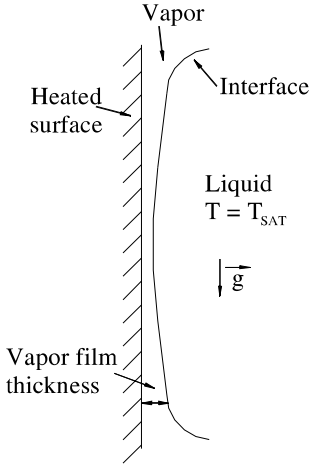

Fig. 1. Vapor–liquid configuration in regions of significant heat transfer (Greitzer and Abernathy).

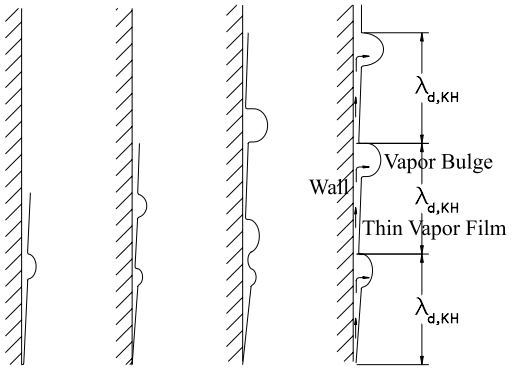

Fig. 2. Vapor unit-film model for film boiling from a vertical surface (Nishio and Ohtake).

the two-dimensional waves which were created in this region, would be developed upward with a constant velocity. The same upper regions were considered as the second section, which consisted of a thin film and a vapor bulge. Since the generated vapor at the thin film was absorbed by the bulge located on the upside of the thin film, the thickness of vapor layer immediately after the bulge would be very thin. Thus the distribution of heat transfer and the length of occupied area by every one of upper regions were the same, and therefore the results of study in one unit could almost be extended to the entire height of surface. Also, the length of each region which was the distance between two consecutive vapor bulges, was considered equal to the most dangerous Kelvin–Helmholtz instability wavelength. This wavelength has been derived analytically by Nishio and Ohtake (1993), based on the instability theory as

$$\lambda_{d,KH} = 16.2\left\{ Pr_{vf}/(S_p^* \cdot Gr_v[\lambda_0]) \right\}^{1/4} \lambda_0 \quad (1)$$

Based on this analytical model, the local Nusselt number has been derived as

$$Nu[\lambda] = 0.74(Gr_v[\lambda] Pr_{vf}/S_p^*)^{1/4} \quad (2)$$

Son and Dhir (1997) carried out a complete numerical simulation of the evolution of vapor–liquid interface, during the saturated film boiling on a horizontal surface. For an axisymmetric case, they used a coordinate transformation technique supplemented by a numerical grid generation method. In this method, the matching conditions at the interface could be imposed accurately, as long as the computational grid could be constructed numerically. From the numerical simulation, the film thickness and, in turn, the heat transfer coefficient were found to vary both spatially and temporally.

Another numerical study of the film boiling, independent of Son and Dhir's (1997) work, was reported by Juric and Tryggvason (1998). They used a two-dimensional front tracking method, which could handle the break-off of interface. In their method, the interface was described as a transition region of finite thickness, rather than as a surface separating the two fluids. Son and Dhir (1998) have simulated the saturated film boiling on a horizontal surface, based on a level set method. This method not only handled the break-off and the merge of interface, but could also be extended easily to three-dimensional problems. The numerical algorithm developed by Sussman et al. (1994) for incompressible two-phase flow was modified to include the effect of liquid–vapor phase change.

The above mentioned level set method was based on a δ-function formulation to enforce the appropriate boundary conditions at the interface. Thus, it smears out any discontinuity in normal velocity, forcing a continuous velocity field across the interface. This numerical smearing could be quite troublesome, introducing divergence into the flow (velocity) field near the interface and, hence, not exactly satisfying the divergence-free condition. This problem was partly solved by Helenbrook et al. (1999) through removing the numerical smearing of the normal velocity obtaining a sharp interface profile. Also, Helenbrook and Law (1999) employed the same approach to obtain results for cases in which the flame fronts (discontinuities) did not merge or become highly curved. These limitations were overcome in the recent work of Nguyen et al. (2001) proposing a new numerical method for treating two-phase incompressible flow. Their method admitted a sharp interface representation similar to the method proposed by Helenbrook et al. (1999). In addition, the interface boundary conditions were handled in a simple fashion such that no special treatment was required to treat the merging of flame fronts.

The objectives of the present work, however, were to extend the modified level set method to encompass the saturated pool film boiling on a vertical surface, and to understand the mechanism of bubble growth, and also, to evaluate the heat transfer adjacent to the hot vertical surface. Hence, some comparisons of the present numerical results with the available experimental and analytical data were performed.

2. Numerical simulation

As mentioned before, the experimental and theoretical studies have showed that the interface waves, which have been developed at the liquid–vapor interface in film boiling on a vertical surface, have divided the region adjacent to the hot surface to similar subregions. Thus, one of these subregions has been evaluated to study the film boiling and the results have extended approximately over the entire surface.

2.1. Assumptions

In the present study, the computations were performed for a two-dimensional incompressible flow, which was described in Cartesian coordinates. The computational domain was chosen as the rectangular regions between the nodes of Kelvin–Helmholtz waves, as shown in Fig. 3. Each rectangle had an area $\lambda_{d,KH}^2/2$, so that the length of the rectangle was assumed as $\lambda_{d,KH}$ along the surface height and parallel to the x-axis, which was located between the nodes of Kelvin–Helmholtz waves, and the width of the rectangle was considered as $\lambda_{d,KH}/2$ perpendicular to the hot surface and parallel to the y-axis.

It was assumed that the fluid properties, including density, viscosity and thermal conductivity, were constant in each phase. Also, the hot surface was assumed flat, vertical and isothermal. The fluid flow adjacent to

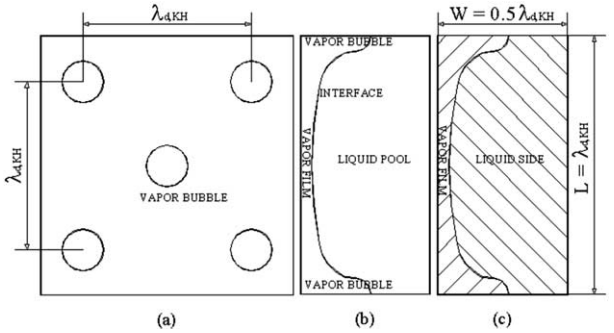

Fig. 3. (a) Vapor bubbles location, (b) interface configuration, and (c) computational domain.

the hot surface was assumed laminar, unsteady and two-dimensional (x, y).

2.2. Governing equations

The interface separating the two phases was captured by a level set function, ϕ, which was defined as a signed distance from the interface: the negative sign was chosen for the vapor phase and the positive sign for the liquid phase. So, the value of $\phi = 0$ stated the interface location. On the basis of the works of Son and Dhir (1998), Sussman et al. (1994) and Chang et al. (1996), the zero level set of ϕ was advanced by the interfacial velocity according to the following equation

$$\phi_t + U_i \cdot \nabla\phi = 0 \tag{3}$$

where U_i is the interfacial velocity vector and it was defined as

$$U_i = U + m/\rho \tag{4}$$

It was derived from the condition of mass continuity and energy balance at the interface

$$m = \rho_v(U_i - U_v) = \rho_l(U_i - U_l) \tag{5}$$

$$m = -K\nabla T/h_{fg} \tag{6}$$

$$(U_i - U_v) = v_{fg}m \tag{7}$$

where $v_{fg} = \rho_v^{-1} - \rho_l^{-1}$. Using Eq. (7) and noting the fact that the mass transfer occurred only at the interface while the phase change process was done, giving the continuity equation as follows

$$\nabla \cdot U = -Km \cdot \nabla H \tag{8}$$

The equations governing the momentum conservation including inertia, pressure, gravity, viscosity and surface tension terms are written as

$$\rho(U_t + U \cdot \nabla U) = -\nabla P + \rho g - \sigma k \nabla H + \nabla \cdot \mu \nabla U \tag{9}$$

In the above equation, H is a step function ($H = 0$ for $\phi < 0$ and $H = 1$ for $\phi > 0$) and k is the interfacial curvature, expressed as follows, according to Brackbill et al. (1992).

$$k = \nabla \cdot (\nabla\phi/|\nabla\phi|) \tag{10}$$

Also, density, viscosity and thermal conductivity are described as

$$\rho = \rho_v + (\rho_l - \rho_v)H \tag{11a}$$

$$\mu_r^{-1} = \mu_v^{-1} + (\mu_l^{-1} - \mu_v^{-1})H \tag{11b}$$

$$K^{-1} = K_v^{-1} + (K_l^{-1} - K_v^{-1})H \tag{11c}$$

To prevent the numerical instability, arising from the discontinuous material properties, the step function was smoothed as

$$\begin{aligned} H &= 1 && \text{if } \phi \geqslant 1.5 \text{ h} \\ &= 0 && \text{if } \phi \leqslant -1.5 \text{ h} \\ &= 0.5 + (\phi/3\text{ h}) + [\sin(2\pi\phi/3\text{ h})]/2\pi && \text{if } |\phi| \leqslant 1.5 \text{ h} \end{aligned} \tag{12}$$

Eq. (12) implied that the interface separating the two phases was replaced by a transition region of finite thickness, in which fluid properties were changed from liquid to vapor as the phase change process was done, according to Eqs. (11a)–(11c).

The energy equation for the film boiling was derived to satisfy the condition that the vapor–liquid interface was maintained at saturation temperature

$$\begin{aligned} &\rho_v C_{Pv}(T_t + U \cdot \nabla T) = \nabla \cdot K\nabla T && (\text{for } H < 1) \\ &T = T_{SAT} && (\text{for } H = 1) \end{aligned} \tag{13}$$

where the effective K was evaluated by setting $K_l^{-1} = 0$ (i.e., no temperature gradient in the liquid) in the Eq. (11c) as

$$K^{-1} = K_v^{-1}(1 - H) \tag{14}$$

2.3. Boundary conditions

The boundary conditions were as follows (see Fig. 4):

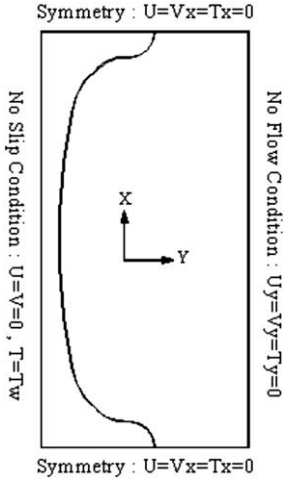

Fig. 4. The boundary conditions.

- At the wall ($y = 0$), no-slip condition: $u = v = 0$; $T = T_W$.
- At the planes of axisymmetry ($x = 0$, $\lambda_{d,KH}$): $u = v_x = T_x = 0$.
- At the end of the computation domain ($y = \lambda_{d,KH}/2$), no-flow condition: $u_y = v_y = T_y = 0$.

2.4. Discretization method and solving procedure

When discretizing the governing equations temporally, the diffusion terms were treated by a fully implicit scheme and the convection and source terms by a first-order explicit method. Also, while discretizing the differential equations spatially, a second-order finite difference method was used (see Fig. 5). Then, the discretized governing equations were expressed as

$$(\phi^{n+1} - \phi^n)/\Delta t + U_i^n \cdot \nabla\phi = 0 \tag{15}$$

$$\nabla \cdot U^{n+1} = v_{fg} m^{n+1} \cdot \nabla H \tag{16}$$

$$\rho(U^{n+1} - U^n)/\Delta t + \rho U^n \cdot \nabla U^n = -\nabla P^{n+1} - \sigma k \nabla H + \rho g + \nabla \cdot \mu \nabla U^{n+1} \tag{17}$$

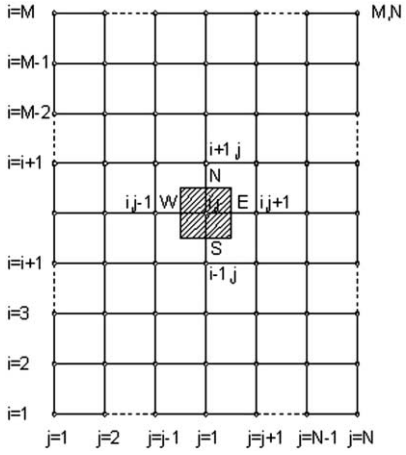

Fig. 5. Grids and the computational cell.

$$\rho_v C_{pv}(T^{n+1} - T^n)/\Delta t + \rho_v C_{pv} U^n \cdot \nabla T^n = \nabla \cdot K \nabla T^{n+1} \tag{18}$$

In order to obtain the governing equation for pressure which achieved the mass conservation, the fractional step method or the projection method, used by Son and Dhir (1998), was employed. In this method, the momentum equation was decomposed into two fractional steps as

$$\rho(U^* - U^n)/\Delta t + \rho U^n \cdot \nabla U^n = -\nabla P^n + \rho g - \sigma k \nabla H + \nabla \cdot \mu \nabla U^* \tag{19}$$

$$U^{n+1} = U^* - \Delta t(\nabla P^{n+1} - \nabla P^n)/\rho \tag{20}$$

First, Eq. (19) was solved using the pressure evaluated at the previous time step. Then, the resulting velocity, U^*, which did not satisfy the continuity equation, was corrected, as given by Eq. (20). When substituting Eq. (20) into Eq. (19), the projection error could be estimated to be $\Delta t(\nabla P^{n+1} - \nabla P^n)/\rho$. Using Eq. (20) and the continuity equation (16), the governing equation for pressure was obtained as

$$\nabla \cdot (\nabla P^{n+1}/\rho) = \nabla \cdot (\nabla P^n/\rho) + (\nabla \cdot U^*/\Delta t) - (v_{gf} m^{n+1} \cdot \nabla H/\Delta t) \tag{21}$$

The discretized equations were solved iteratively by a line-by-line tridiagonal-matrix algorithm (TDMA) supplemented by the Gauss–Seidel method, which was suggested by Patankar (1980).

Based on the above assumptions and according to the procedure which was developed in this work, the computations were performed as shown in Fig. 6.

3. Results and discussion

The special case for performing the computations, is the standard condition for boiling with $T_{SAT} = 100$ °C and $P_{atm} = 100$ KPa. Also, another important quantity

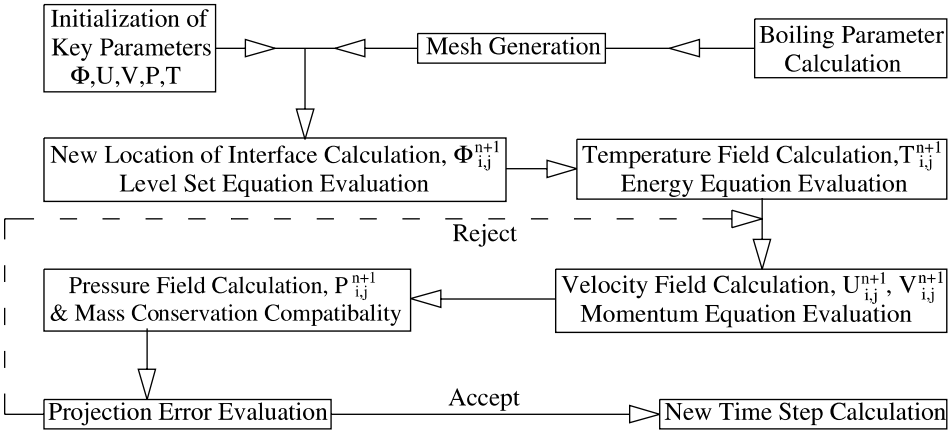

Fig. 6. The flow diagram of solution algorithm for modified level set method.

which affected the film boiling phenomenon was the saturated temperature difference, ΔT. In the present study, computations were performed for various ΔT and the important parameters related to boiling were computed, as presented in the following figures.

The computation domain was comforted with a uniform mesh to discretize the governing equations. It was found that a 256×128 grid would give the appropriate results.

The time steps were chosen so as to satisfy the Courant–Friedrichs–Lewy (CFL) condition (Anderson, 1995), which was stated as $\Delta T \leqslant (|U|/\Delta X + |V|/\Delta Y)$. In this study, it was found that an appropriate time step was approximately a dimensionless time of 0.01. To perform the computations, a computer code was developed in Microsoft Fortran Power Station (4) environment.

Fig. 7 shows the interface location and configuration at various time steps for $T_W = 250$ °C, which from the qualifying view point the numerical results were similar to the previous theoretical studies such as those of Bui and Dhir (1985), Nishio and Ohtake (1993) and Son and Dhir (1998). Also, according to this figure the thin vapor film and the vapor bubbles are visible and the distance between bubbles were became exactly equal to $\lambda_{d,KH}$ in agreement with existing analytical models.

Fig. 8 illustrates the temperature field at 5th time step for $T_W = 250$ °C, where the temperature contours were the same as expected, such that with distancing from the

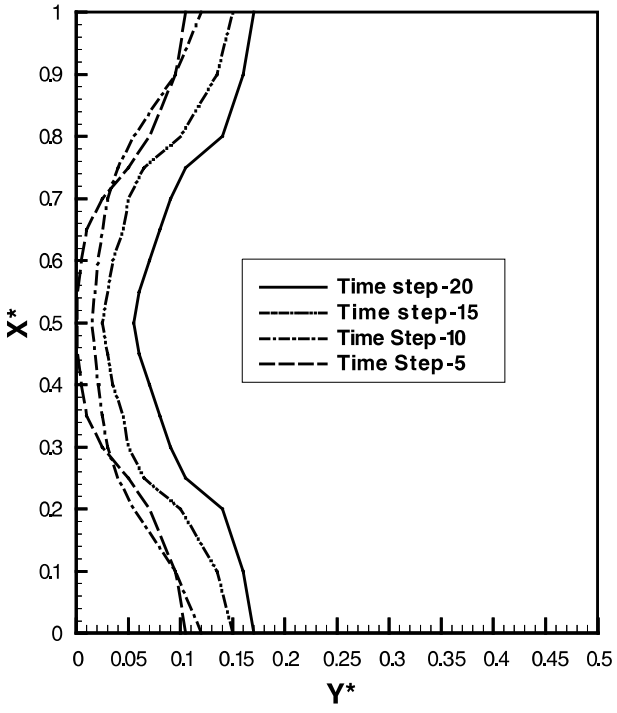

Fig. 7. Liquid–vapor interface at 5th, 10th, 15th and 20th time steps for $T_W = 250$ °C.

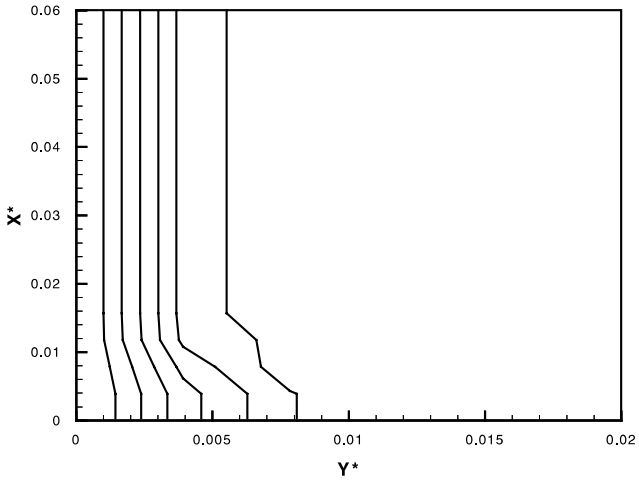

Fig. 8. Temperature contours at 5th time step for $T_W = 250$ °C.

interface, the isothermal lines were parallel with the interface, and in the thin vapor film region, these lines are vertical and also, in the vapor bubbles the curvature of isothermal lines are the same as the interface.

The velocity field at 5th time step for $T_W = 250$ °C is shown in Fig. 9. It can be seen that the flow vectors in the liquid and vapor phases were as expected, such that the direction of flow in the vapor region is from the thin vapor film to the vapor bubbles. Therefore, the numerical results were in agreement with the model proposed by Bui and Dhir (1985), based on the empirical observations. Also, it can be concluded that, the phase change process from liquid to vapor was performed in the thin vapor film and the vapor would transfer from this region to the bubbles which acted as a reservoir.

The results of old theories were in the form of the Nusselt number as a function of distance from the lower edge of vertical surface, but, in disagreement with those, the experimental studies showed that this dependence would be decreased with the distance from the lower edge of surface, and gradually would become negligible. Fig. 10 Shows the Nusselt number versus the height of surface. According to this diagram, *Nu* remained almost constant along the height of surface, which, was in agreement with the experimental observations. But, because *Nu* was defined as a dimensionless temperature gradient adjacent to the hot surface, and since the vapor layer was more thick in bubbles, therefore, the temperature gradient in this region was lower and naturally, *Nu* was also lower in the bubbles.

Fig. 11 demonstrates the average heat transfer coefficient versus ΔT, where the present numerical results have been compared with the existing analytical theory predictions. The comparisons showed differences in the order of 5–35%. These differences were increased with ΔT growth. The very simplifying assumptions which were considered in the first two models (Bui and Dhir, 1985; Koh, 1962), could cause the difference with the

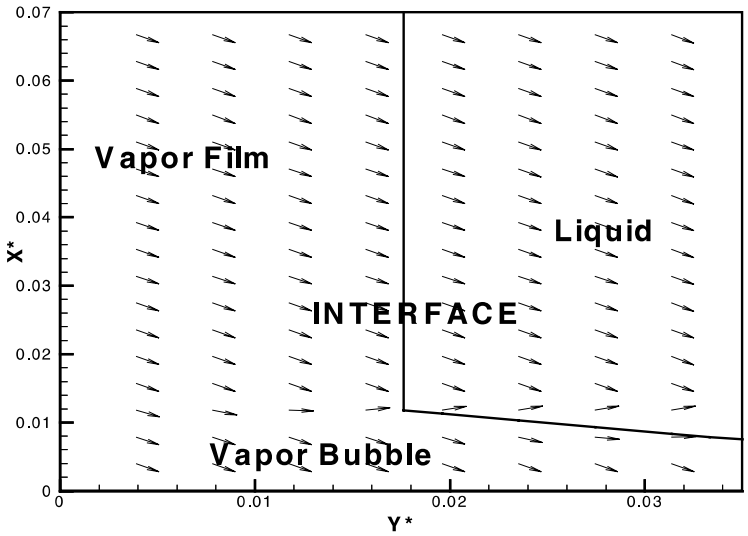

Fig. 9. Velocity field at 5th time step For $T_W = 250$ °C.

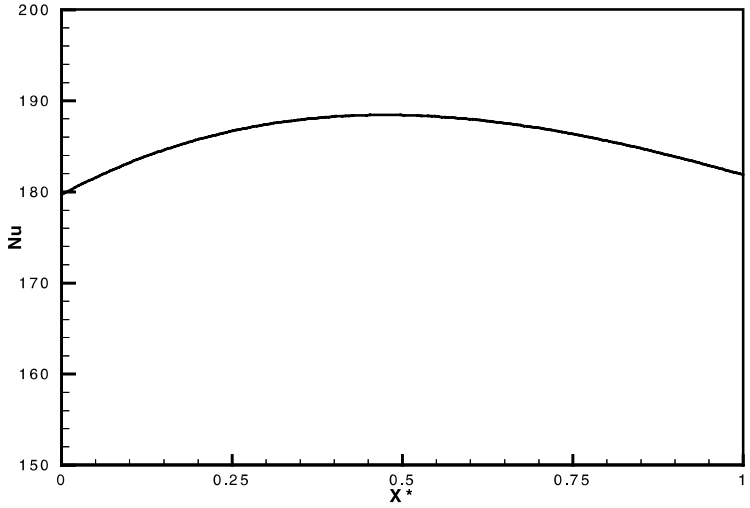

Fig. 10. Time average Nusselt number for $T_W = 250$ °C.

present numerical results. Some of the assumptions were as follows: Koh's (1962) model: A smooth vapor–liquid interface was considered without accounting for the interface waves effects and, also, the process was assumed as steady with a stable laminar vapor film. Bui and Dhir's (1985) model: The inertia effects in the vapor film were not accounted for and also, only the conductive heat transfer was considered in the vapor bubbles.

Therefore, the overestimation of the present numerical results in comparison with the analytical models was reasonably acceptable. On the other hand, Greitzer and Abernathy's (1972) model was closer to the present numerical results. Because, as was described in Section 1, this analytical model was proposed based on a qualifying evaluation of the governing equations of the vapor film, which was converted to the exact equations by the interpolation method, based on some experimental data. Thus, the results obtained from this model were more reliable and its closer agreement with the present numerical results could state the validity of the present numerical analysis.

Finally, the heat flux at the hot surface is shown in Fig. 12, where the present numerical results have been compared with the available experimental data of Bui and Dhir (1985). It can be seen that the overall trend is similar and as in Fig. 11 the difference between the numerical and the experimental results was increased with ΔT growth. But, a 25–40% difference existed, which would be expected as there were differences between the experimental conditions and the numerical computations, including the constant fluid properties and the two-dimensional flow assumptions which were considered in the present numerical analysis.

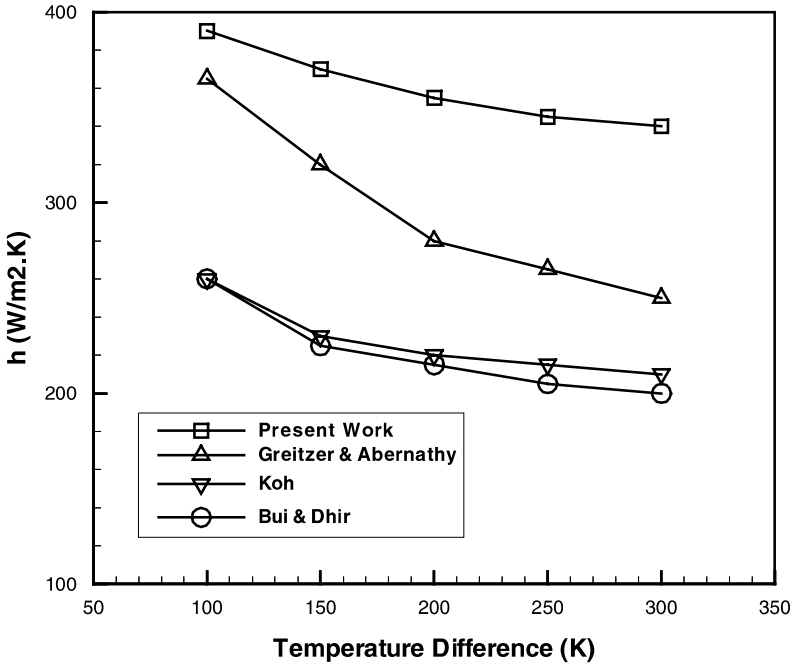

Fig. 11. Comparisons of present heat transfer coefficient results with others.

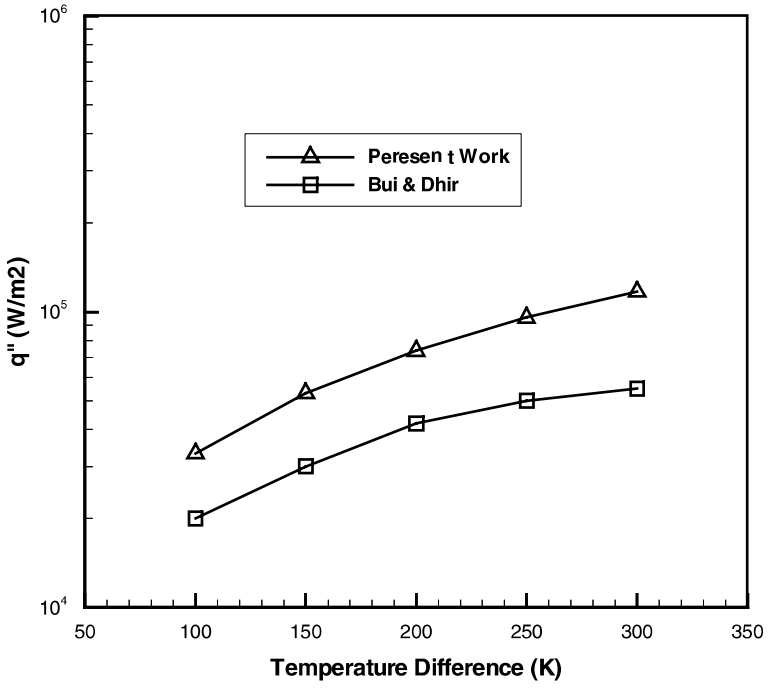

Fig. 12. Comparison of present heat flux results with experimental data of Bui and Dhir.

4. Conclusion

The heat transfer coefficient results obtained from the present numerical work were compared with the available analytical and experimental results and a reasonable agreement was shown. Also, it can be concluded that the modified level set method has been relatively successful to evaluate the saturated film boiling process. Overall, the film boiling is a very complicated phenomenon, because there are a lot of variations of the fluid properties adjacent to two sides of the interface. If one could apply a more exact and high order discretization method, along with a smaller grid, some better results would be expected. Also, the introduction of more

realistic models as well as the implementation of fluid property variations, in the vapor phase, could possibly lead to better future simulations.

References

Anderson, J.D., 1995. Computational Fluid Dynamics—The Basics with Applications. McGraw-Hill, New york.

Brackbill, J.U., Kothe, D.B., Zemach, C., 1992. A continuum method for modeling surface tension. J. Computat. Phys. 100, 335–354.

Bromley, L.A., 1950. Heat transfer in stable film boiling. Chem. Eng. Prog. 46, 221–227.

Bui, T.D., Dhir, V.K., 1985. Film boiling heat transfer on an isothermal vertical surface. ASME J. Heat Transfer 107, 764–771.

Chang, Y.C., Hou, T.Y., Merriman, B., Osher, S., 1996. A level set formulation of Eulerian interface capturing methods for incompressible fluid flow. J. Computat. Phys. 124, 449–464.

Greitzer, E.M., Abernathy, F.H., 1972. Film boiling on vertical surfaces. Int. J. Heat Mass Transfer 15, 475–491.

Helenbrook, B.T., Law, C.K., 1999. The role of Landau–Darrieus instability in large scale flows. Combustion Flame 117, 155–169.

Helenbrook, B.T., Martinelli, L., Law, C.K., 1999. A numerical method for solving incompressible flow problems with a surface of discontinuity. J. Comput. Phys. 148, 366–396.

Juric, D., Tryggvason, G., 1998. Computations of boiling flows. Int. J. Multiphase Flow 24 (3), 387–410.

Koh, J.C.J., 1962. Analysis of film boiling on vertical surfaces. ASME J. Heat Transfer 84 (1), 55–62.

Nguyen, D.Q., Fedkiw, R.P., Kang, M., 2001. A boundary condition capturing method for incompressible flame discontinuities. J. Comput. Phys. 172, 71–98.

Nishio, S., Ohtake, H., 1993. Vapor-film-unit model and heat transfer correlation for natural-convection film boiling with wave motion under subcooled condition. Int. J. Heat Mass Transfer 36 (10), 2541–2552.

Patankar, S.V., 1980. Numerical Heat Transfer and Fluid Flow. Hemisphere Publishing, New York.

Son, G., Dhir, V.K., 1997. Numerical simulation of saturated film boiling on an horizontal surface. ASME J. Heat Transfer 119, 225–533.

Son, G., Dhir, V.K., 1998. Numerical simulation of film boiling near critical pressure with a level set method. ASME J. Heat Transfer 107, 764–771.

Sussman, M., Smereka, P., Osher, S., 1994. A level set approach for computing solutions to incompressible two-phase flow. J. Comput. Phys. 114, 146–459.